Climate and Economics: Tropical Forests
Part III

Centre for microdata methods and practice - UCL - April 2024

April 24, 2024

Motivation: Flying Rivers

- Trees recycle humidity back to atmosphere, Salati et al. [1979]
- Generate "flying rivers" that are responsible for ∼30-40% of rain in Amazon
- Rainfall → trees' transpiration → recharges atmospheric humidity → humidity moves downwind → rainfall.
- Less trees → less water downwind. Deforestation → degradation.
- Rain is responsible for rain-forest
- Rain-forest is also responsible for the rain.
- More water in flying rivers than in the Amazon River.
- Photos by Sebastião Salgado.

Estimating spatial amplification of degradation of Amazon I

- Araujo et al. [2023]
- In addition to local impacts, human-induced disturbances of forest are likely to cascade following the eastern-western atmospheric flow generated by trade winds.
    - No trees, no humidity recycling.
- Model spatial and temporal interactions created by this flow to estimate spread of effects to downwind locations.
- Spatial component captures cascading effects propagated by neighboring regions while temporal component captures the persistence of local disturbances.
- Estimate that on average, the presence of cascading effects mediated by winds in the Amazon doubles the impact of an initial damage.

Estimating spatial amplification of degradation of Amazon II

- Heterogeneity: damage in some regions does not propagate. In others amplification can reach 250%.
- Only account for spillovers mediated by wind ⇒ underestimation of spillovers.

Related literature I

- Water recycling in Amazon: Salati et al. [1979], Costa et al. [2012]
- Large-scale calibrated models connecting forest dynamics and climate to construct scenarios of forest resilience *e.g.,* Shukla et al. [1990],Wunderling et al. [2022], Nobre et al. [1991] (see Araujo et al. [2023] for additional references)
- Research focused on measuring resilience indicators such as changes in status of vegetation Boulton et al. [2022], in net carbon emissions Gatti et al. [2021], or in rainfall regime Salati et al. [1979](See additional references in Araujo et al. [2023].)
- Araujo [2023] also uses wind data but does not measure cascading effects.

Related literature II

- Using reduced form econometric methods to answer questions in climate science:
- Artic Sea Ice Diebold and Rudebusch [2022], Diebold et al. [2022].
- Goal of Araujo et al. [2023] is to make explicit identification hypothesis to establish causal effect and enhance interpretation of estimates.
    - Counterfactuals

Mechanisms and model

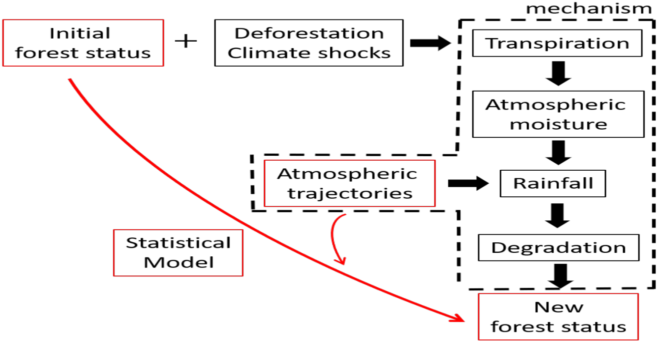

- Statistical model abstract from transpiration mechanism; uses variations on atmospheric trajectory to estimate dynamics

Atmospheric trajectories I

- Need to identify immediate neighbors and measure atmospheric trajectories that transport humidity
  - Pixel resolution determined by wind data - 0.25° resolution ($\sim 27.5km^2$ near equator)
  - Relevant wind is at 800hPa ($\sim$ 6000 feet) [Spracklen et al., 2012].
- Let G be a matrix such that $G_{ij} = 1$ if and only if pixels i and j are immediate neighbors. Otherwise $G_{ij} = 0$
- Let $C_{ij,t} = 1$ if a trajectory of atmospheric circulation at t goes through j before reaching i. Otherwise $C_{ij,t} = 0$.
- Let $W_t = G \odot C_t$, $w_{ij,t} = G_{ij} C_{ij,t} \in \{0, 1\}$ equals 1 if pixel j has **direct** effect on i via atmospheric circulation at time t.
- W_t is "climate adjacency matrix".
- $\odot$ indicates Hadamard (componentwise) product

Atmospheric trajectories II

- $$\hat{W}_t^{[k]} := \left(\mathbb{I}(G^k > 0) - \sum_{j=1}^{k-1} \mathbb{I}(G^j > 0) \right) \odot C_t$$
- $(W_t^{[k]})_{ij} := (\hat{W}_t^{[k]})_{ij}$, if $i \neq j$ and $(W_t^{[k]})_{ii} := 0$.
- $W_t^{[k]}$ as the matrix of kth-degree neighbors. $W_t^{[k]}$ identifies pixels i and j that are k-th degree geographical neighbors *and* are connected through atmospheric circulation at t.
- $W^{[1]} := W$
- To build back-trajectories of wind over time, use monthly three-dimensional wind data (direction and speed) from 1985 to 2013 (Copernicus [2017]). For each pixel, trace back the trajectory that arrives at that pixel at 800 hPa ($\sim 6000 feet$) for 5 days; enough for back-trajectories to reach ocean.

Atmospheric trajectories III

- Identification assumption: $(W_t^{[k]})_{ij}(W_t^{[k]})_{ji} = 0$.
  - Physics: Wind in Amazon goes southwest (Heat gradient plus Coriolis effect)
  - Verified in data.

Illustration

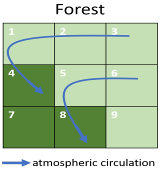

$C_t =$

	1	2	3	4	5	6	7	8	9
1	0	1	1	0	0	0	0	0	0
2	0	0	1	0	0	0	0	0	0
3	0	0	0	0	0	0	0	0	0
4	1	1	1	0	0	0	0	0	0
5	0	0	0	0	0	1	0	0	0
6	0	0	0	0	0	0	0	0	0
7	0	0	0	0	0	0	0	0	0
8	0	0	0	0	1	1	0	0	0
9	0	0	0	0	0	0	0	0	0

$G =$

	1	2	3	4	5	6	7	8	9
1	0	1	0	1	1	0	0	0	0
2	1	0	1	1	1	1	0	0	0
3	0	1	0	0	1	1	0	0	0
4	1	1	0	0	1	0	1	1	0
5	1	1	1	1	0	1	1	1	1
6	0	1	1	0	1	0	0	1	1
7	0	0	0	1	1	0	0	1	0
8	0	0	0	1	1	1	1	0	1
9	0	0	0	0	1	1	0	1	0

$Y_t =$

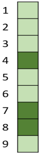

$W_t =$

	1	2	3	4	5	6	7	8	9
1	0	1	0	0	0	0	0	0	0
2	0	0	1	0	0	0	0	0	0
3	0	0	0	0	0	0	0	0	0
4	1	1	0	0	0	0	0	0	0
5	0	0	0	0	0	1	0	0	0
6	0	0	0	0	0	0	0	0	0
7	0	0	0	0	0	0	0	0	0
8	0	0	0	0	1	1	0	0	0
9	0	0	0	0	0	0	0	0	0

$W_t^{[2]} =$

	1	2	3	4	5	6	7	8	9
1	0	0	1	0	0	0	0	0	0
2	0	0	0	0	0	0	0	0	0
3	0	0	0	0	0	0	0	0	0
4	0	0	1	0	0	0	0	0	0
5	0	0	0	0	0	0	0	0	0
6	0	0	0	0	0	0	0	0	0
7	0	0	0	0	0	0	0	0	0
8	0	0	0	0	0	0	0	0	0
9	0	0	0	0	0	0	0	0	0

- Y_t vector of pixels LAI at t. C_t shows for each row-pixel, pixels that affect it. $G_{ij} = 1$ if pixels (i, j) are immediate geographical neighbors.

Leaf area index I

- Leaf area index (LAI) is a dimensionless quantity that measures the amount of leaf area in a plant canopy
- LAI= Leaf area/ground area
  - Leaf area is one sided.
- Provides information on density and extent of vegetation cover. Higher LAI value indicates denser canopy with more leaves, which can result in increased photosynthesis, carbon sequestration, biomass production, and overall productivity.
- Higher frequency fluctuations
- Affected by seasons.
- LAI data from the NOAA Climate Data Record of AVHRR Leaf Area Index (LAI) at the spatial resolution of 0.05° for 1985-2013 Claverie et al. [2016].

Leaf area index II

- Longest LAI time-series available; includes decades of high deforestation rates.

- Reduce LAI's data resolution to wind-data resolution applying an average kernel.

Model I

- Y_t vector of LAI indices of pixels.
- Specify the evolution of forest status as a spatial dynamic panel:

$$Y_t = \alpha Y_{t-1} + \sum_{k=1}^{K} \beta_k W_t^{[k]} Y_t + X\gamma + \varepsilon_t \tag{1}$$

- X vector of pixel characteristics
- Equation (1) is a consistency (equilibrium) requirement for cross-section of LAI, given previous LAI and shocks.
    - 5 days are enough for air parcel to travel entire Amazon
    - t is monthly
- Since dynamic panel use first differences

$$\Delta Y_t = \alpha \Delta Y_{t-1} + \sum_{k=1}^{K} \beta_k \Delta(W_t^{[k]} Y_t) + \tilde{\varepsilon}_t \tag{2}$$

Model II

- Use Y_{t-2} as instrument for ΔY_{t-1} because Y_{t-1} is correlated with $\tilde{\varepsilon}_t$
- See Arellano [1989], Phillips and Han [2015]
- To avoid the effects of anthropogenic processes that affect simultaneously several pixels, instrument $\Delta(W_t^{[k]} Y_t)$ by $\Delta W_t^{[k]} Y_0$.
- Thus use the following $K+1$ moment conditions to identify parameters.

$$\mathbb{E}\left[\tilde{\epsilon_t} Y_{t-2}\right] = 0 \tag{3}$$

$$\mathbb{E}\left[\tilde{\epsilon_t} \Delta(W_t^{[k]} Y_0)\right] = 0 \tag{4}$$

- No over-identifying restrictions.

Estimates: α

- Standard errors clustered at the pixel level. Number of observations: 3,300,494. Number of clusters: 9,539
- $\alpha = .22$ (.0019)
- Persistence coefficient higher than average persistence of individual effects computed by Boulton et al. [2022], but within within 1sd bounds of these individual coefficients.
- α should be interpreted as partial persistence coefficient after controlling for state of rest of forest.
- Therefore low α does not imply that forest state has low persistence.

Estimates: β

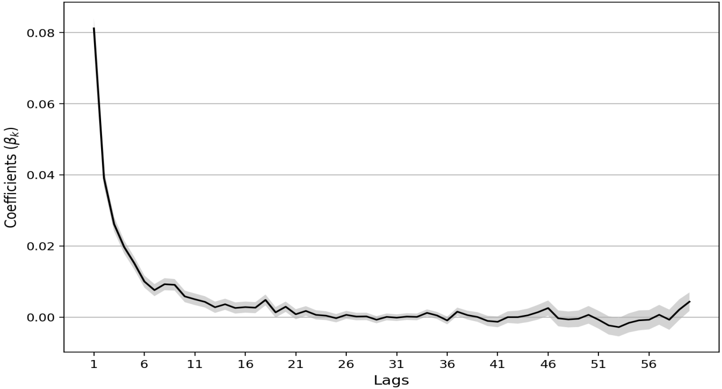

- $\sum_{k=1}^{20} \beta_k = .26$

Additional controls?

- Possible causal chain of effects: (a) a decrease in upwind LAI leads to (b) a decrease in precipitation downwind and (c) an increase in fire vulnerability downwind, thus (d) decreasing downwind LAI.
- Instead of breaking down the mechanism as $(a) \rightarrow (b) \rightarrow (c) \rightarrow (d)$ we estimate directly $(a) \rightarrow (d)$.
- Including precipitation and/or fire as controls would keep important mechanisms constant or block their path of causality, thereby absorbing the variation necessary to estimate the model.
- " Bad controls," Wooldridge [2005], Angrist and Pischke [2009]
- "Mediators", Cinelli et al. [2022]

Impulse response I

- There are many ways to define impulse-responses
- $W^{[k]} := \frac{1}{T}\sum_t W_t^{[k]}$, T time-length of data.
  - Process of atmospheric transport is mean-ergodic
  - Sample average ($W^{[k]}$) representative of future patterns.
- $\Omega := \left(I - \sum_{k=1}^{K} \beta_k W^{[k]}\right)^{-1}$.
  - Summarizes in a single matrix all average feedback effects of the spatial dimension.
- If $||W|| < 1$ and $K = 1$,
  $\Omega = (I - \beta_1 W)^{-1} = I + \beta_1 W + \beta_1^2 W^2 + \beta_1^3 W^3 + \ldots$.
- $$Y_t = \alpha \Omega Y_{t-1} + \Omega X \gamma + \Omega \epsilon_t$$

Impulse response II

- May also iterate for a time window Δ,

$$Y_{t+\Delta} = \alpha^{\Delta+1}\Omega^{\Delta+1}Y_{t-1} + \sum_{i=0}^{\Delta}\alpha^{i}\Omega^{i+1}X\gamma + \sum_{i=0}^{\Delta}\alpha^{i}\Omega^{i+1}\epsilon_{t+\Delta-i} \quad (5)$$

- Using previous estimates we can calculate an impulse response function ϕ

$$\phi(t+\Delta) := \alpha^{\Delta}\mathbb{I}_{row}\left(\Omega^{\Delta+1}\epsilon_t\right) \quad (6)$$

  - $\mathbb{I}_{row}$ denote a row vector of ones
- $(\phi(t+\Delta))$ returns the effect that a shock ϵ_t at time t, has on the forest status over all pixels at $t+\Delta$, for an average pattern of atmospheric situation.
  - The effect is linear on the initial shock

Impulse response III

- Aggregate effect of a unit shock to pixel i on the forest, after an interval of time Δ, is the sum of the elements in row i of the matrix $\Omega^{\Delta+1}$.
- Analogously, the effect of a unit shock to all pixels on site j is given by the sum of the entries in column j of the matrix $\Omega^{\Delta+1}$.
- As $\Delta \to 0$, effect of a unit shock ϵ^i in site i on forest is given by $\sum_j \Omega_{ij}$
    - *Index of influence* of i
- $\sum_i \Omega_{ij}$
    - *Index of exposure* of j
- As Δ increases, matrix $\Omega^{\Delta+1}$ decays fast and most influential pixels move to north-northeast accompanying the inverse trajectory of trade winds.

A: Index of influence B: Index of exposure

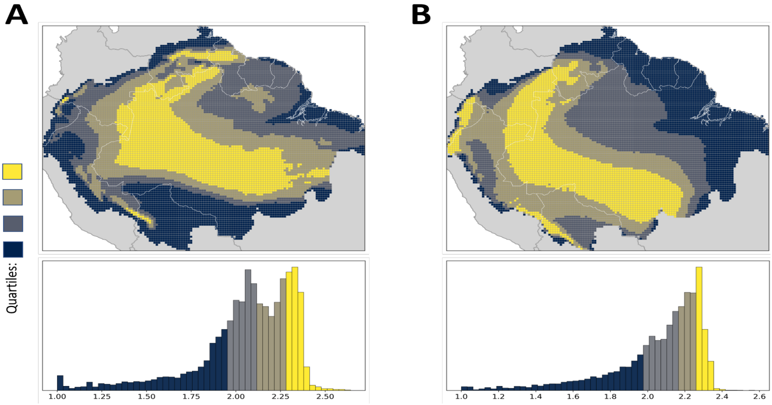

- Average multiplier is 2.

Predicted LAI effect of most deforested pixels

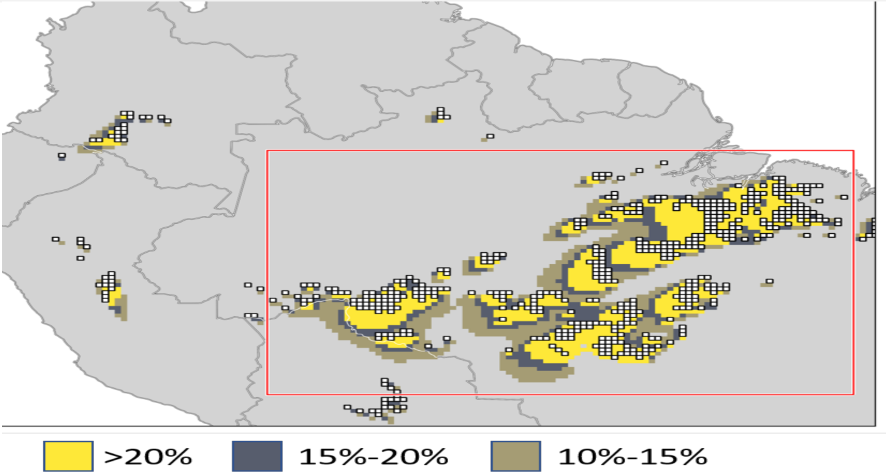

- White pixels are pixels that were deforested at least 50% in 2001-2022.

Transnational externality

- Effect of deforestation in pixels in Rondonia state.

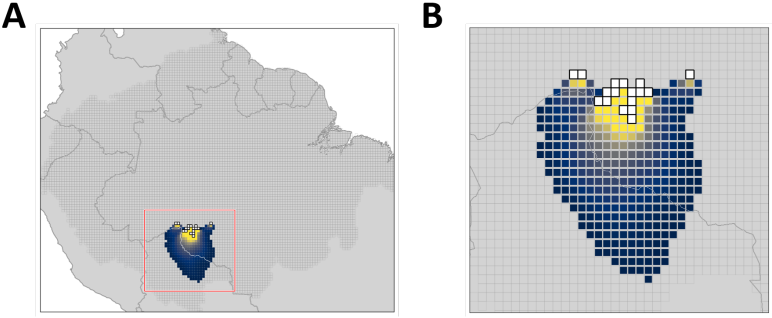

Conclusions

- Identified important externalities of forest degradation.
- Can identify crucial pixels.*
- To apply to model such as in Assunção et al. [2023] need to obtain "price" of LAI
- Connect changes in LAI to changes in carbon.
- Reduced LAI increases local temperature.
- Regression of ΔCO_2 on ΔLAI and interactions of ΔLAI interacted with LON, LAT and $Lon \times LAT$ restricted to sites with $\Delta LAI < 0$ has negative coefficient that is significant
- Point estimates similar and better R^2 if restrict to $\Delta LAI < -5\%$
- No causality

References I

JD Angrist and JS Pischke. Mostly harmless econometrics: An empiricist's guide p. 373. 2009.

Rafael Araujo. When clouds go dry: An integrated model of deforestation, rainfall, and agriculture. 2023.

Rafael Araujo, Juliano Assunção, Marina Hirota, and José A Scheinkman. Estimating the spatial amplification of damage caused by degradation in the amazon. *Proceedings of the National Academy of Sciences*, 120 (46):e2312451120, 2023.

Manuel Arellano. A note on the anderson-hsiao estimator for panel data. *Economics letters*, 31(4):337–341, 1989.

Juliano J Assunção, Lars Peter Hansen, Todd Munson, and José A Scheinkman. Carbon prices and forest preservation over space and time in the brazilian amazon. *Available at SSRN 4414217*, 2023.

References II

Chris A Boulton, Timothy M Lenton, and Niklas Boers. Pronounced loss of amazon rainforest resilience since the early 2000s. *Nature Climate Change*, 12(3):271–278, 2022.

Carlos Cinelli, Andrew Forney, and Judea Pearl. A crash course in good and bad controls. *Sociological Methods & Research*, page 00491241221099552, 2022.

Martin Claverie, Jessica L Matthews, Eric F Vermote, and Christopher O Justice. A 30+ year avhrr lai and fapar climate data record: Algorithm description and validation. *Remote Sensing*, 8(3):263, 2016.

Climate Change Service Copernicus. Era5: Fifth generation of ecmwf atmospheric reanalyses of the global climate. 2017.

References III

Marcos H. Costa, Laura Borma, Paulo M. Brando, José A. Marengo, Scott R. Saleska, and Gatti Luciana V. Biogeophysical cycles: Water recycling, climate regulation. *Science Panel for the Amazon.*, Chapter 7, 2012.

Francis X Diebold and Glenn D Rudebusch. Probability assessments of an ice-free arctic: Comparing statistical and climate model projections. *Journal of Econometrics*, 231(2):520–534, 2022.

Francis X Diebold, Glenn D Rudebusch, Maximilian Göbel, Philippe Goulet Coulombe, and Boyuan Zhang. When will arctic sea ice disappear? projections of area, extent, thickness, and volume. Technical report, National Bureau of Economic Research, 2022.

References IV

Luciana V Gatti, Luana S Basso, John B Miller, Manuel Gloor, Lucas Gatti Domingues, Henrique LG Cassol, Graciela Tejada, Luiz EOC Aragão, Carlos Nobre, Wouter Peters, et al. Amazonia as a carbon source linked to deforestation and climate change. *Nature*, 595(7867): 388–393, 2021.

Carlos A Nobre, Piers J Sellers, and Jagadish Shukla. Amazonian deforestation and regional climate change. *Journal of climate*, 4(10): 957–988, 1991.

Peter CB Phillips and Chirok Han. The true limit distributions of the anderson–hsiao iv estimators in panel autoregression. *Economics Letters*, 127:89–92, 2015.

Eneas Salati, Attilio Dall'Olio, Eiichi Matsui, and Joel R Gat. Recycling of water in the amazon basin: an isotopic study. *Water resources research*, 15(5):1250–1258, 1979.

References V

Jagadish Shukla, Carlos Nobre, and Piers Sellers. Amazon deforestation and climate change. *Science*, 247(4948):1322–1325, 1990.

Dominick V Spracklen, Steve R Arnold, and CM Taylor. Observations of increased tropical rainfall preceded by air passage over forests. *Nature*, 489(7415):282–285, 2012.

Jeffrey M Wooldridge. Violating ignorability of treatment by controlling for too many factors. *Econometric Theory*, 21(5):1026–1028, 2005.

Nico Wunderling, Arie Staal, Boris Sakschewski, Marina Hirota, Obbe A Tuinenburg, Jonathan F Donges, Henrique MJ Barbosa, and Ricarda Winkelmann. Recurrent droughts increase risk of cascading tipping events by outpacing adaptive capacities in the amazon rainforest. *Proceedings of the National Academy of Sciences*, 119(32): e2120777119, 2022.